Formation of New Thermosets by the Reaction of Cyanates with Thiophenols

Monika Bauer,[1] Jörg Bauer[2]

[1]*Fraunhofer Research Institution for Polymeric Materials and Composites, Kantstrasse 55, D-14513 Teltow, Germany*
[2]*Fraunhofer Institute for Reliability and Microintegration, Gustav-Meyer-Allee 25, D-13355 Berlin, Germany*

Received 3 July 2007; accepted 26 February 2008
DOI 10.1002/app.28430
Published online 11 June 2008 in Wiley InterScience (www.interscience.wiley.com).

ABSTRACT: Sulfur-containing aromatic thermosets, mainly consisting of aryloxy- and arylthio-substituted 1,3,5-triazines, have been prepared through the reaction of difunctional cyanates with mono- and difunctional aromatic thiols. A straightforward three-step reaction scheme is proposed and verified by the identification of key substances: (1) the addition of thiol and cyanate groups, (2) the stepwise addition of (thio)imino carbonic esters with one another, and (3) the ring closure of chain-extended (thio)imino carbonic esters to form 1,3,5-triazines. Reactions of types 2 and 3 are associated with an abstraction of phenol or thiophenol, which can enter into reaction 1 again. Characterization of the curing behavior of dicyanate of bisphenol A with thiophenol as well as dimercaptodiphenyl sulfide by differential scanning calorimetry shows that the reaction rates are significantly enhanced by the admixture of thiols to the cyanate. Dynamic mechanical analysis of resulting thermosets showed that large amounts of comonomers can be incorporated into the network resulting in a decrease of glass temperature but increase of fracture toughness. Finally, the fully cured thermosets resulting from the reaction of dicyanate of bisphenol A with different admixtures of dimercaptodiphenyl sulfide were characterized by cone calorimetry to get information about flame retardancy. The flame retardancy is influenced by incorporation of dimercaptodiphenyl sulfide into the triazine network only slightly. © 2008 Wiley Periodicals, Inc. J Appl Polym Sci 110: 8–17, 2008

Key words: flame retardance; mechanical properties; step-growth polymerization; structure–property relations; thermosets

INTRODUCTION

Thermosets, formed by polycyclotrimerization of di- and polyfunctional cyanates and their modifications with other monomers, are of increasing importance for all kinds of applications because of their excellent properties. In particular, excellent thermomechanical properties and good fire retardancy are the reasons for their high application potential in aircraft. Because of the need to balance the properties for each application (side-wall panel, fuselage, etc.), coreactions are used to meet the required properties.

Investigations of the reactions of aromatic cyanic acid esters (cyanates) with a large number of functional groups were started immediately after their first successful synthesis in the 1960s. Among other things, special interest was focused on nucleophilic addition, in which many substances with mobile hydrogen atoms were found to react straightforwardly with the cyanate group.[1,2] In this way, thiophenols (TPs) were added to cyanates to form thioimino carbonic esters.[1–4] The reactions were performed at moderate temperatures in solution with a variety of solvents. Additionally, the abstraction of phenol from the thioimino carbonic ester and the formation of the thiocyanate were described by Grigat and Pütter.[3] The reaction conditions were similar, but the reaction temperature was slightly higher. Up to now, no reactions in bulk have been described, and no results for di- or multifunctional compounds that are able to form thermosets have been reported.

In this study, we investigated the buildup of sulfur-containing aromatic thermosets using the reaction in bulk of difunctional cyanates and mono- and difunctional aromatic thiols. First, monofunctional model compounds [4-*tert*-butyl phenyl cyanate (4tbPC) and TP] were used to elucidate the main chemical structures with the help of high-performance liquid chromatography (HPLC), matrix-assisted laser desorption/ionization time-of-flight spectroscopy (MALDI-TOF), and Fourier transform infrared (FTIR). The network buildup resulting from the reaction in bulk of the difunctional cyanate 2,2-bis-(4-cyanatophenyl)-propane [dicyanate of bisphenol A (DCBA)] with TP was also analyzed by MALDI-TOF. Finally, the curing behavior and thermomechanical properties of copolymers of DCBA with mono- and difunctional thiols were characterized with dynamic mechanical analysis (DMA) and differential scanning calorimetry (DSC).

Correspondence to: M. Bauer (monika.bauer@pyco.fraunhofer.de).

Contract grant sponsor: Fonds der Chemischen Industrie.

EXPERIMENTAL

Materials

4-*tert*-Butylphenol (4tbP), TP, diphenyl disulfide (DPDS), and 4,4′-dimercaptodiphenyl sulfide (DMDPS) were purchased from Sigma–Aldrich Chemie GmbH (TaufKirchen, Germany) and had purities greater than 98%. The monofunctional cyanate 4tbPC was synthesized from the corresponding phenol 4tbP with the bromocyan method[5] and distilled twice *in vacuo* to get a purity greater than 99% (HPLC). DCBA (Primaset B10) was obtained from Lonza GmbH (Wuppertal, Germany) and had a purity greater than 99%.

Reactions

Reactions of approximately 1 g of 4tbPC with different amounts of TP were carried out in small cylindrical glass tubes placed in an oil bath. The mixtures were cured isothermally for 4 h at 150°C. Reactions with DCBA were performed in the same way at 150°C but stopped just before gelation occurred. The obtained mixtures were analyzed with HPLC, MALDI-TOF, and FTIR.

Castings (60 × 10 × 4 mm) were prepared in aluminum sheet molds from degassed mixtures of DCBA with several amounts of TP or DMDPS. Curing was done isothermally at 120°C until vitrification, and then further isothermal curing steps were applied in 20° steps up to 220°C. The curing times for the isothermal steps were 1 h, and the heating rates between these isothermal steps were kept low (<1 K/min) to prevent exothermal heating. The obtained samples were analyzed by DMA.

Liquid chromatography

HPLC was performed with equipment including two WellChrom Maxi-Star K-1000 high-pressure pumps (Knauer GmbH, Berlin, Germany), an analytical ultraviolet–visible detector, an electrically driven injection valve, and the software package EuroChrom 2000 from Knauer (Berlin, Germany). Steel columns (250 × 4-mm i.d.) filled with endcapped Eurospher C18 (particle diameter = 5 μm, pore diameter = 100 Å) were used for separations. The mobile phase, acetonitrile/water, was degassed before the measurements.

MALDI-TOF

MALDI-TOF measurements were performed with a Kratos Kompakt MALDI III from Kratos Analytical (Manchester, UK). A sample (1.6 mg) and 6.4 mg of dithranol (1,8,9-trihydroxyanthracene) as a matrix were dissolved in 1 mL of tetrahydrofuran and measured in a linear mode to get the mass spectrum of the sample.

FTIR spectroscopy

FTIR measurements were performed with an FTS 165 spectrometer from Bio-Rad (Hercules, CA). Samples were dissolved in methylene chloride, dropped on a 3M Teflon card from Spectra-Tech, Inc. (Oak-Bridge, TN), and dried at room temperature. Spectra were recorded directly from the cards, and background spectra were taken from the neat cards.

DSC

DSC measurements were performed with a PL-DSC from Rheometrics Scientific (München, Germany). The substances were mixed separately, and 5–10 mg of each sample was placed in Al pans and sealed. Scanning experiments were performed at heating rates of 2, 5, 10, and 20 K/min.

DMA

Rectangular bars were cut from the castings and measured in torsion in a forced vibration mode at 1 Hz with a torsional dynamic mechanical spectrometer from Polymer Laboratories (Shropshire, UK). After a first run up to a temperature about 50 K higher than the glass transition, a second run was performed to detect the postcure and to measure fully cured systems.

Fracture toughness

The fracture toughness, that is, the critical mode I stress intensity factor, was measured with compact tension (CT) specimens (W = 35) cut from the castings with a CNC milling machine. An Instron 4456 electromechanical testing machine (Canton, MA) was used at a crosshead speed of 1 mm/min for the fracture toughness tests. Tests were performed according to ASTM Standard D 4045 but extended over the scope of the standard with an optical method of monitoring crack propagation (called optical crack tracing). Thus, fracture toughness was measured not only for crack initiation but also for crack propagation (i.e., the R-curve was measured). The main advantage of measuring the R-curve is that fracture toughness for crack initiation is often measured too high because of imperfect precracks (giving mode II contributions), but fracture toughness measured for crack propagation still gives the intrinsic mode I fracture toughness (because the crack approaches the path of least energy during propagation, i.e., mode I); that is, the accuracy is much higher, and fewer samples can be used.

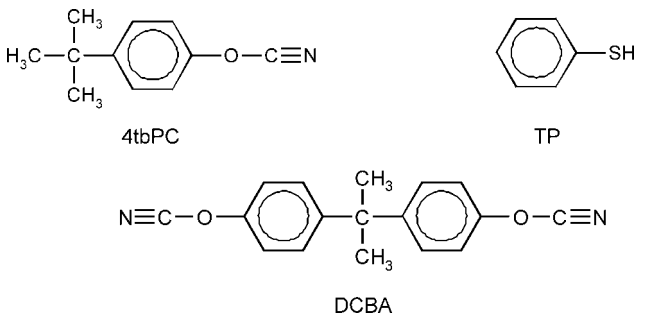

Scheme 1 Structures of the substances.

Cone calorimetry

The heat release rate and smoke evolution were investigated with a cone calorimeter from Fire Testing Technology, Ltd. (East Grinstead, West Sussex, UK) Samples (60 mm^2) with a thickness of 5 mm were tested at a heat flux of 50 kW/m^2. The volume flow of the exhaust gases was 24 L/s. The scanning interval of the data was 3 s. A steel frame with an inner opening of 60 × 60 mm^2 was used to protect sample edges during the test instead of a standard retainer frame. Unexposed sample surfaces were wrapped in aluminum foil.

RESULTS AND DISCUSSION

Monofunctional model compounds 4tbPC and TP were used to elucidate, via HPLC, MALDI-TOF, and FTIR, the main chemical structures resulting from the reaction in bulk of cyanate esters and aromatic thiols. The applicability of the derived reaction scheme to the network buildup of difunctional cyanate esters and thiols was then proved by an analysis of the oligomeric products of the reaction in bulk of difunctional DCBA and TP. The chemical structures of the used monomers are shown in Scheme 1.

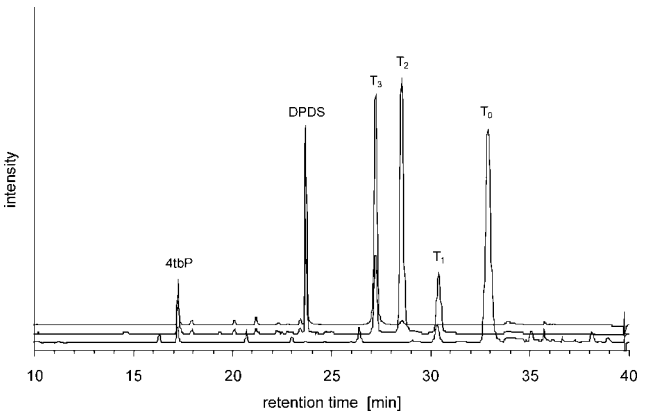

Figure 1 Chromatograms of three reaction mixtures of 4tbBP and TP with different initial compositions after 4 h at 150°C (SH fraction = 1, 50, or 70 mol % from bottom to top).

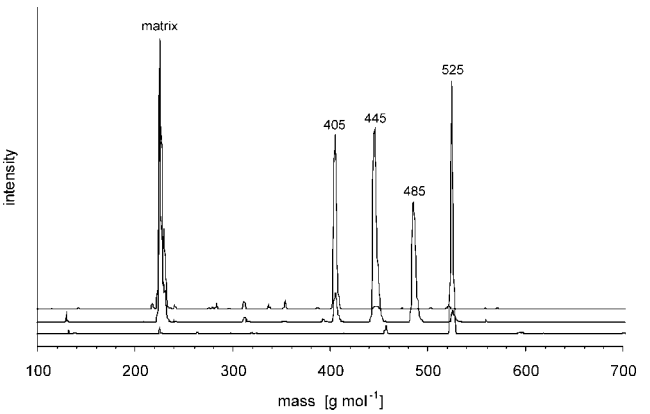

Figure 2 MALDI-TOF spectra of three reaction mixtures of 4tbBP and TP with different initial compositions after 4 h at 150°C (for the lines, see Fig. 1).

Reactions of 4tbPC with TP

TP was added to the cyanate 4tbPC in different molar fractions ranging from 1 to 80 mol %. The mixtures reacted for 4 h at 150°C without any solvent or catalyst. The resulting reaction products were analyzed by HPLC and MALDI-TOF; three examples of low, medium, and high contents of TP are plotted in Figures 1 (HPLC) and 2 (MALDI-TOF). The complete conversion of all cyanate groups was checked by FTIR, for which the disappearance of the characteristic OCN valance vibration between 2200 and 2350 cm^{-1} was used as an indicator.[6,7] The measured FTIR spectra of a mixture with 50 mol % TP after mixing and after the reaction are shown in Figure 3 as examples.

Three reaction products were easily identified by the use of HPLC with the help of reference compounds: 4tbP with a retention time of 17.3 min, DPDS with a retention time of 23.8 min, and the trimerized cyanate 2,4,6-tris-(4-*tert*-butylphenoxy)-1,3,5-triazine (T_0) with a retention time of 33.2 min (see Fig. 1 and Scheme 2). On the other hand, 4tbPC

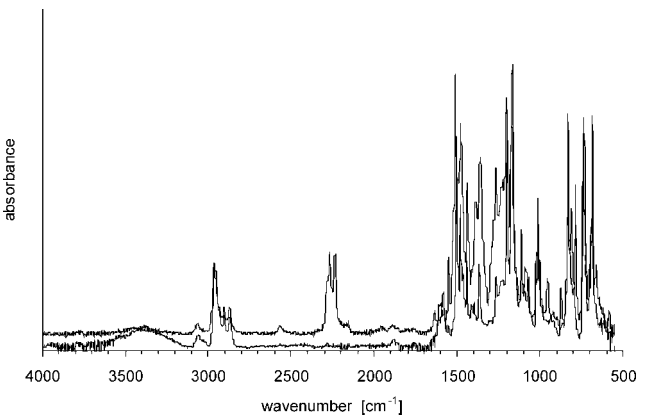

Figure 3 IR spectra of a mixture of 4tbBP and 50 mol % TP after mixing (top) and after 4 h at 150°C (bottom).

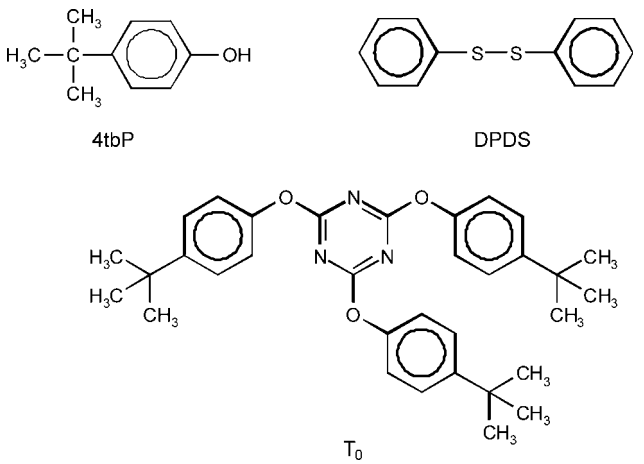

Scheme 2 Structures of the found reaction products.

(retention time = 21.0 min) was completely consumed in all samples, and this confirmed the full conversion of cyanate groups after the reaction was finished.

Besides, MALDI-TOF and HPLC analyses of the reaction mixtures showed only a few other products. The main HPLC peaks with retention times of 30.5, 28.8, and 27.4 min were isolated by preparative HPLC and measured by MALDI-TOF. Their masses of 485, 445, and 405 g/mol exactly corresponded to the masses of the main peaks of the MALDI spectra of the whole reaction mixtures, for which the peak at 525 g/mol was already identified as trimer T_0. The remaining structures could be related to the three analogous triazine structures T_1, T_2, and T_3 with increasing substitution of 4-*tert*-butylphenyl by thiophenyl (see Scheme 3).

Basic reactions

The formation of triazine structures with various substituents can be explained by a mechanism that is similar to one found for the reaction of cyanate esters with phenols.[6] The first step is the addition of a cyanate ester (R—OCN) and a thiol (R′—SH) to form the thioimino carbonic ester **1** (see Scheme 4).

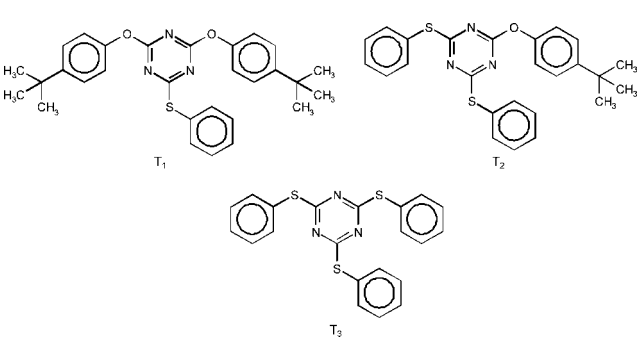

Scheme 3 Structures of the found substituted triazines.

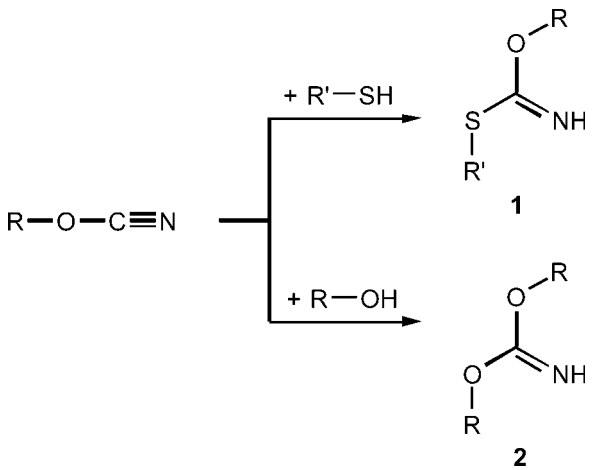

Scheme 4 Addition of thiols or phenols with cyanate esters.

R and R′ represent the main structures of general cyanate and thiol molecules (R = 4-*tert*-butylphenyl and R′ = phenyl for the substances used in this study). The same type of reaction also happens between R—OCN and R—OH (4tbP in this study) and yields the imino carbonic ester **2**. R—OH is formed by the abstraction reaction (see Scheme 5 or 6).

Reactive species **1** and **2** are key products for the proceeding steps of the reaction. They react immediately under the applied reaction conditions with another (thio)imino carbonic ester (**1** or **2**) to form the intermediates **3a**, **3b**, and **3c**, which differ in the number and position of aryloxy or arylthio substituents (see Scheme 5). Here, the structure of the resulting species **3a**, **3b**, or **3c** depends not only on the structure of the starting molecules (**1** or **2**) but also

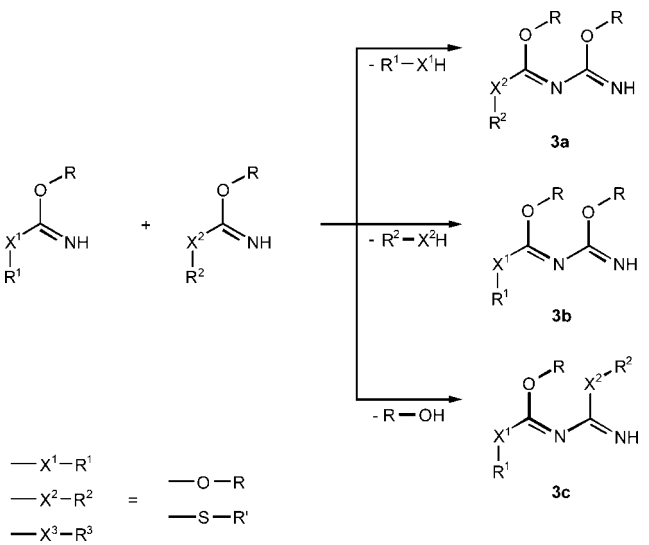

Scheme 5 Stepwise addition of (thio)imino carbonic esters with one another (the XR substituents are defined in Scheme 6).

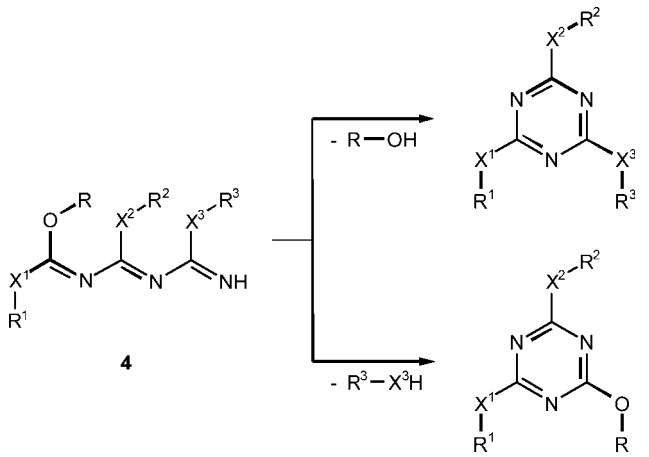

Scheme 6 Ring closure and formation of triazines.

on the type of abstracted moiety (R—OH or R′—SH). The abstracted phenol or TP can then enter the starting reaction again (see Scheme 4).

The same type of reaction can take place in a proceeding step by the addition of one molecule of **1** or **2** and one molecule of **3a**, **3b**, or **3c**, resulting in a species of the general structure **4** (see Scheme 6) and an abstracted phenol or TP, which can enter the starting reaction (see Scheme 4). Molecules of type **4** easily stabilize by ring formation and abstraction of a phenol or thiol into the found aryloxy/arylthio-substituted triazine T_0, T_1, T_2, or T_3 (see Scheme 6).

The proposed reaction scheme, which is based on thioimino and imino carbonic ester structures as reactive species, straightforwardly explains the formation of all four possible differently substituted triazines found experimentally and is consistent with the analogous reactions of cyanates with phenols[6,7] and amines,[8] respectively. The formation of triazines having more than one arylthio substituent (T_2 and T_3) cannot be explained by the alternative mechanism, which is based on a stepwise addition of cyanates instead of (thio)imino carbonic ester **1** or **2**.

According to the reaction scheme, the initially used molar fraction of TP exists in two forms in the final state: as TP again, being abstracted according to Scheme 5 or 6, or as a substituent of a triazine of type T_1, T_2, or T_3, in which the same number of phenolic molecules is abstracted. This is confirmed by the identification of the phenol 4tbP as well as DPDS instead of free TP in the reaction mixtures with the help of HPLC and MALDI-TOF (Figs. 1 and 2). DPDS was formed from two molecules of TP according to the well-known disulfide bridge reaction.

Quantitative distribution of the reaction products

The chromatograms were also analyzed quantitatively to determine the distribution of the products in the final stage of the reactions. The needed calibration factors were determined with the help of chromatograms of different concentrations of reference compounds 4tbP, DPDS, T_0, T_1, T_2, and T_3, for which pure samples of the triazines were obtained by preparative HPLC. In this way, concentrations of moles of a certain species per gram of the mixture were determined, which could be rearranged to get the normalized molar concentration of the relevant structural elements:

$$[R_T] = 3[T_0] + 2[T_1] + [T_2] \quad (1)$$

$$[R'_T] = 3[T_3] + 2[T_2] + [T_1] \quad (2)$$

$$[R] = [4tbP] + [R_T] \quad (3)$$

$$[R'] = 2[DPDS] + [R'_T] \quad (4)$$

where the 4-*tert*-butylphenyl structure of R—OCN is denoted by R and the phenyl structure of R′—SH is denoted by R′. $[R_T]$ is the molar concentration of R linked to a triazine, $[R'_T]$ is the molar concentration of R′ linked to a triazine, [R] is the molar concentration of all R, and [R′] is the molar concentration of all R′. The molar concentrations in eqs. (1)–(4) are normalized for [R] + [R′] = 100%, so the concentrations describe the percentage distributions of R and R′ among the different reaction products.

Figure 4 shows the obtained fractions of different triazines with respect to the initial molar fraction of TP. High yields of T_0 were obtained only at low contents of TP, whereas the fraction of T_0 rapidly decreased with an increasing initial molar fraction of TP; this indicated a high level of arylthio substitution. A preferred buildup of the mixed triazines T_1

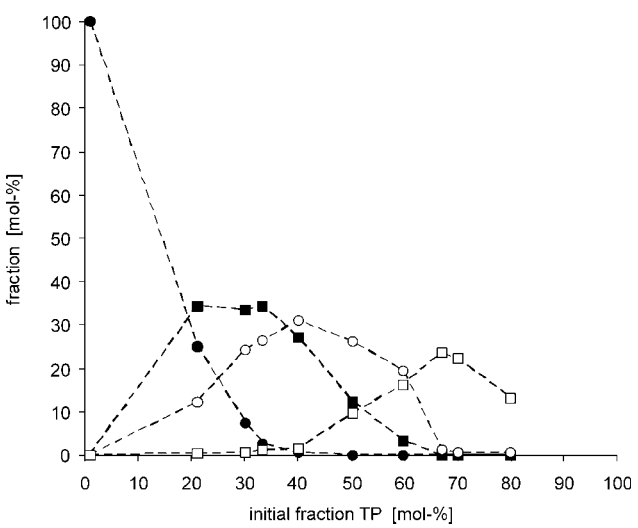

Figure 4 Fraction of triazines after 4 h at 150°C versus the initial molar fraction of TP determined by HPLC: (●) T_0, (■) T_1, (○) T_2, and (□) T_3.

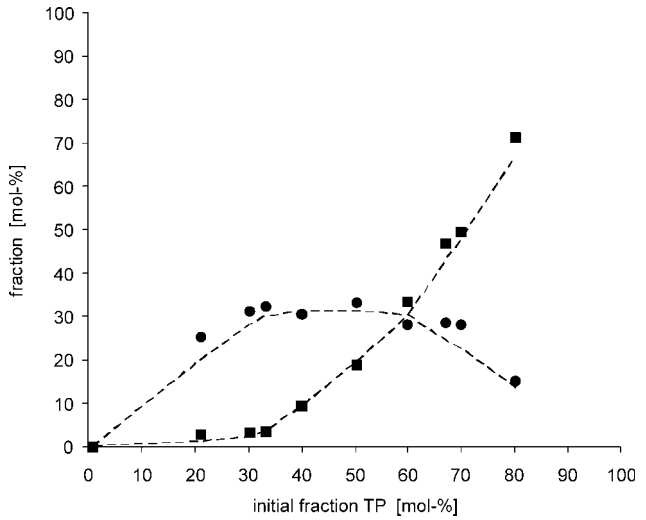

Figure 5 Fractions of (●) 4tbP and (■) DPDS after 4 h at 150°C versus the initial molar fraction of TP determined by HPLC. The lines were calculated from HPLC according to eqs. (5) and (6).

and T_2 was found in a wide intermediate range of initial cyanate/thiol mixing ratios, and only the completely arylthio-substituted triazine T_3 was formed above an initial TP fraction of about 70 mol %.

Measured fractions of 4tbp and DPDS are plotted in Figure 5 versus the initial molar fraction of TP. The fraction of DPDS monotonically increased with an increasing initial molar fraction of TP as expected. On the other hand, the fraction of 4tbP increased, remained at a nearly constant level in a wide intermediate range, and decreased at high initial molar fractions of TP. This is plausible because high fractions of TP cause low fractions of 4tbPC from which only low fractions of 4tbP can be formed.

The proposed reaction mechanism suggests a close connection between the fractional distribution of the triazines T_0, T_1, T_2, and T_3 and the fractions of 4tbP and DPDS. According to Schemes 4–6, any insertion of R′ into a triazine causes an abstraction of R, which yields 4tbP:

$$[R_{4tbP}] = [R'_T] \tag{5}$$

where $[R_{4tbP}]$ is the molar concentration of R in 4tbP. Furthermore, any unreacted or abstracted R′, which is not a substituent of a triazine, forms DPDS because no free TP was found in the final stage of reaction:

$$[R'_{DPDS}] = [R']_0 - [R'_T] \tag{6}$$

where $[R'_{DPDS}]$ is the molar concentration of R′ in DPDS and $[R']_0$ is equivalent to the initial molar fraction of TP. Figure 5 shows that the calculated fractions $[R_{4tbP}]$ and $[R'_{DPDS}]$ are in very good agreement with the measured values of the 4tbP and DPDS concentrations.

It is plausible that the upper limit of R'_T is equal to the initial molar fraction of TP as long as $[R']_0$ is less than $[R]_0$ until 50 mol %. On the other hand, the upper limit of R'_T is equal to the initial molar fraction of 4tbPC above this range because every R'_T needs a CN group of a triazine, which stems from a cyanate group:

$$[R_T]_{max} = [R]_0 - [R'_T]_{max} \tag{7}$$

$$[R'_T]_{max} = \min([R]_0, [R']_0) \tag{8}$$

where $[R_T]_{max}$ is the maximum molar concentration of R linked to a triazine and $[R'_T]_{max}$ is the maximum molar concentration of R′ linked to a triazine. The lines representing eqs. (7) and (8) are plotted in Figure 6 together with the measured values calculated according to eqs. (1) and (2). Nearly the whole possible amount of R′ is linked to triazines at low initial molar fractions of TP until about 33 mol %. Simultaneously, the same amount of R is abstracted to form 4tbP. On the other hand, the increasing formation of DPDS from TP and the increasing competition between abstracted 4tbP and TP to add to 4tbPC at intermediate and high initial fractions of TP lead to reduced formation of R'_T below the possible maximum value.

Reactions of DCBA with TP

Polyfunctional cyanates also form a three-dimensional polymer network by polycyclotrimerization in the presence of monofunctional coreagents such as cyanates or phenols, as shown in ref. 6. TP should have a similar effect on the cyanate network buildup

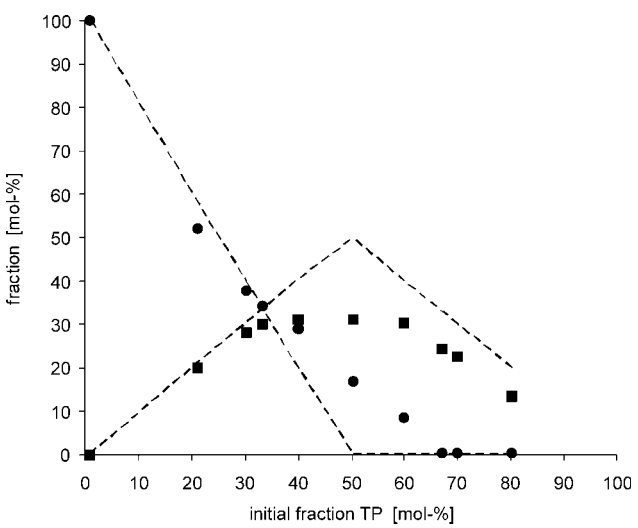

Figure 6 Fractions of (●) R and (■) R′ linked to triazines after 4 h at 150°C versus the initial molar fraction of TP calculated from HPLC according to eqs. (1) and (2). The lines were calculated according to eqs. (7) and (8).

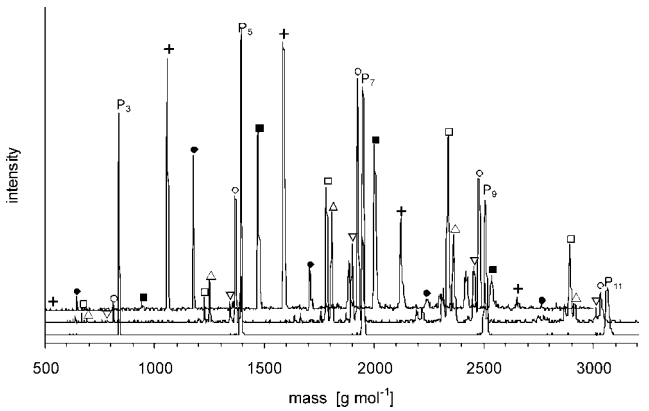

Figure 7 MALDI-TOF spectra of three reaction mixtures of DCBA and TP with different initial compositions after a reaction at 150°C (SH fraction = 1, 20, or 50 mol % from bottom to top; for the marked peaks, see Tables I and II).

if we assume that the straightforward and quick reaction found for the monofunctional cyanate ester 4tbPC with TP (Schemes 4–6) follows the same route with the difunctional cyanate monomer DCBA. To prove this assumption, TP was added to the cyanate DCBA in different molar fractions ranging from 1 to 50 mol %, and reactions were carried out at 150°C without any solvent or catalyst. The reactions were stopped before gelation occurred to get completely soluble samples, which were analyzed by MALDI-TOF; three examples of low, medium, and high contents of TP are plotted in Figure 7.

The measurements show that very low admixtures of TP, such as 1 mol %, lead to a nearly selective polycyclotrimerization of the cyanate: only neat DCBA oligomers consisting of an odd number of DCBA constituting units were found; the oligomers P_3, P_5, P_7, P_9, and P_{11} are marked in Figure 7. All these oligomers consist of $n \geq 1$ triazine rings, $n + 2$ DCBA units as substituents in the 2-, 4-, or 6-position of the triazine rings (TS_1 in Scheme 7), and $n - 1$ DCBA links between two triazine rings (TS_2 in Scheme 7). The compositions and molar masses of the oligomers marked in Figure 7 are listed in Table I; the number of TS_1 units corresponds to the number of unreacted cyanate groups.

Higher admixtures of TP lead to a large number of new reaction products (see Fig. 7), which can be grouped according to their structure. The first group is directly derived from the neat DCBA oligomers P_3, P_5, P_7, and so forth by the substitution of some or all unreacted cyanate groups (TS_1 substituents in Scheme 7) by hydroxyl groups (TS_3 substituents in Scheme 7). Examples of such structural series are marked in Figure 7 (○ and ▽) and are listed in Table I. The formation of TS_3 substituents can be easily explained with the derived reaction scheme: (1) by abstraction of the corresponding TS_1 structure as

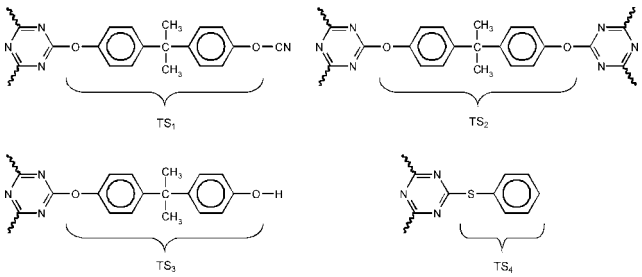

Scheme 7 Substituents of triazine rings during the reaction of DCBA with TP.

a result of an addition step or a ring closure (Scheme 6) or (2) by incorporation of a preformed OH group of bisphenol A or monocyanate of bisphenol A [2-(4-cyanatophenyl)-2-(4-hydroxyphenyl)-propane] as a result of the triazine formation of the second group of the difunctional molecule. According to the reaction scheme, the generation of phenolic OH groups is associated with the formation of a arylthio-substitution TS_4 (see Scheme 7). Thus, not only the identified DCBA oligomers bearing OH end groups but also DCBA/TP co-oligomers should be present in the reaction mixture. Table II gives an overview of five different series of such oligomers. They consist like the neat DCBA oligomers of $n \geq 1$ triazine rings and $n - 1$ DCBA links between two triazine rings (TS_2 in Scheme 7), but the remaining $n + 2$ substituents in the 2-, 4-, or 6-position of the triazine rings are composed of all three possible types: TS_1, TS_3, and TS (see Scheme 7). The molecules listed in Table II are all identified in the MALDI spectra of the reaction mixtures and are marked in Figure 7 according to their structure.

TABLE I
Compositions of the DCBA Oligomers

	Number				
Molar mass (g/mol)	Triazines	TS_1	TS_2	TS_3	TS_4
Oligomers without OH end groups (P_1–P_{11})					
835	1	3	0	0	0
1392	2	4	1	0	0
1948	3	5	2	0	0
2505	4	6	3	0	0
3061	5	7	4	0	0
Oligomers with one OH end group (○)					
810	1	2	0	1	0
1367	2	3	1	1	0
1923	3	4	2	1	0
2480	4	5	3	1	0
3036	5	6	4	1	0
Oligomers with two OH end groups (▽)					
785	1	1	0	2	0
1342	2	2	1	2	0
1898	3	3	2	2	0
2455	4	4	3	2	0
3011	5	5	4	2	0

TABLE II
Compositions of the DCBA/TP Oligomers

	Number				
Molar mass (g/mol)	Triazines	TS_1	TS_2	TS_3	TS_4
Oligomers with one TP and without OH end groups (△)					
692	1	2	0	0	1
1248	2	3	1	0	1
1805	3	4	2	0	1
2362	4	5	3	0	1
2918	5	6	4	0	1
Oligomers with one TP and one OH end group (□)					
667	1	1	0	1	1
1223	2	2	1	1	1
1780	3	3	2	1	1
2337	4	4	3	1	1
2893	5	5	4	1	1
Oligomers with one TP and without OCN end groups (●)					
642	1	0	0	2	1
1173	2	0	1	3	1
1705	3	0	2	4	1
2237	4	0	3	5	1
2768	5	0	4	6	1
Oligomers with two TPs and without OCN end groups (◆)					
524	1	0	0	1	2
1055	2	0	1	2	2
1587	3	0	2	3	2
2118	4	0	3	4	2
2650	5	0	4	5	2
Oligomers with three TPs and without OCN end groups (■)					
406	1	0	0	0	3
937	2	0	1	1	3
1469	3	0	2	2	3
2000	4	0	3	3	3
2532	5	0	4	4	3

The reaction mixture with the 20 mol % initial TP fraction mainly contains neat DCBA oligomers (P_x, ○ and ▽) and DCBA/TP co-oligomers with low contents of TP substituents (△ and □). On the other hand, oligomers with a high degree of TP and TS_3 substituents (●, +, and ■) become dominant in the spectra of reaction mixtures with a large initial TP fraction (e.g., the 50 mol % spectrum in Fig. 7).

In summary, the analysis of the reaction mixtures of DCBA with TP completely confirmed the reaction scheme derived with the help of monofunctional compounds. Thus, TPs can be incorporated to a great extent into cyanurate networks, and phenolic OH end groups of network chains are formed simultaneously.

Thermomechanical properties

Combinations of difunctional DCBA and monofunctional TP as well as difunctional DMDPS have been used to synthesize three-dimensional polymer networks. As shown previously, the DCBA/TP network consists of elements of TS_2, TS_3, and TS_4 (see Fig. 7) at full OCN conversion, whereas the use of difunctional DMDPS instead of TP gives additional structural elements according to the reaction scheme (see Scheme 8): DMDPS with only one reacted functional group forms $TS_{4'}$, a dangling network end with a free thiol group, and connections between triazine rings can also be formed by DMDPS units of TS_5. Thus, three-dimensional polymer networks built up from these units consist at full cure of branching points, triazines with three substitutions of TS_2 or TS_5, chain segments, triazines with two substitutions of TS_2 or TS_5 and one substitution of TS_3 or TS_4 ($TS_{4'}$), dangling chain ends, triazines with one substitution of TS_2 or TS_5 and two substitutions of TS_3 or TS_4 ($TS_{4'}$), low-molecular-weight byproducts, and triazines with three TS_3 or TS_4 ($TS_{4'}$) substitutions.

DMA measurements were performed on thermoset samples prepared from DCBA with different amounts of TP and DMDPS to characterize the thermomechanical properties and to evaluate the effects of the kinds and amounts of the comonomers. The measured DMA spectra (see Fig. 8) show that the modulus in the glassy state is nearly independent of the composition, whereas the moduli above the glass transition decrease significantly for mixtures with higher contents of thiol comonomers. Simultaneously, the α-relaxation range becomes broader, indicating a larger diversity of structural elements.

The effect of changing the structural composition on the thermomechanical properties becomes clearer by a comparison of the measured glass temperatures (see Fig. 9). Obviously, the glass temperatures decrease with increasing amounts of the TP or DMDPS comonomer because the relative content of network branching points, triazine rings with three connections to other triazines, decreases. This effect is more pronounced for admixtures of monofunctional TP because one thiol group produces one network chain end by incorporating the TP molecule into the network (TS_4 in Scheme 7) and another chain end (TS_3 in Scheme 7) by the resulting OH abstraction (see Schemes 5 and 6). On the other hand, a difunctional DMDPS builds a network link (TS_5 in Scheme 8) because in the final state of the reaction nearly all thiol groups are connected with triazines for low admixtures of thiol groups, as shown previously(see Fig. 6). Thus, the amount of unreacted SH ($TS_{4'}$ in Scheme 8) should be low, and network chain ends are formed only by OH abstraction and the resulting structural elements of TS_3 (see

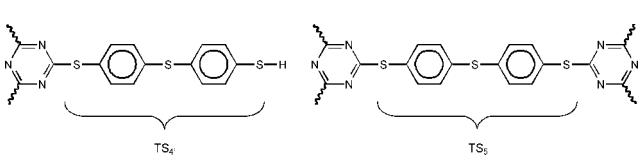

Scheme 8 Substituents of triazine rings during the reaction of DCBA with DMDPS.

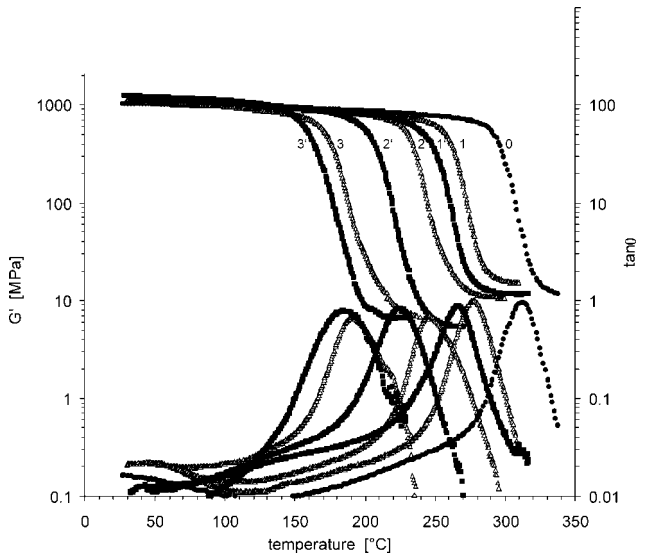

Figure 8 DMA spectra of DCBA-based thermosets at full conversion: (●,0) neat DCBA, (△) DCBA/TP [initial SH content = (1) 2.6, (2) 5.3, or (3) 11.1 mol %], and (■) DCBA/DMDPS [initial SH content = (1′) 5, (2′) 10, and (3′) 20 mol %]. G' is the storage modulus.

Scheme 7). Furthermore, the incorporation of DMDPS into the network and the resulting decrease of the branching density lead not only to a decrease of the glass temperature but also to an increase of toughness.

Curing kinetics

The curing reaction of DCBA with thiol containing comonomers DMDPS and TP was followed by DSC at a heating rate of 10 K/min; measured curves are plotted in Figures 10 and 11. The admixture of thiol groups leads to a shift of the exothermic DSC peaks to lower temperatures, and this indicates a significant increase in the curing rates.

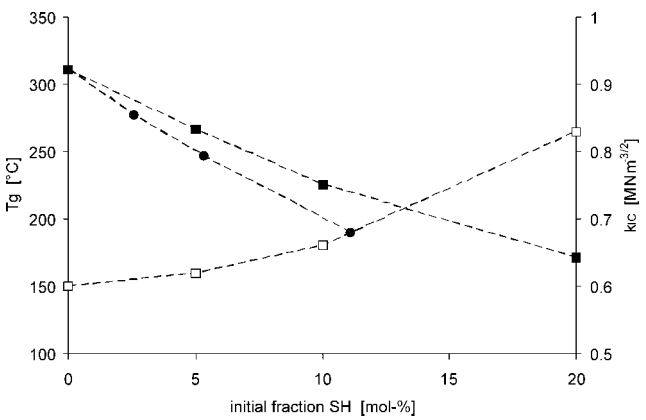

Figure 9 (●,■) Glass-transition temperature (T_g) by DMA and (□) critical mode I stress intensity factor (k_{IC}) of (●) DCBA/TP- and (■,□) DCBA/DMDPS-based thermosets at full conversion versus the initial SH content.

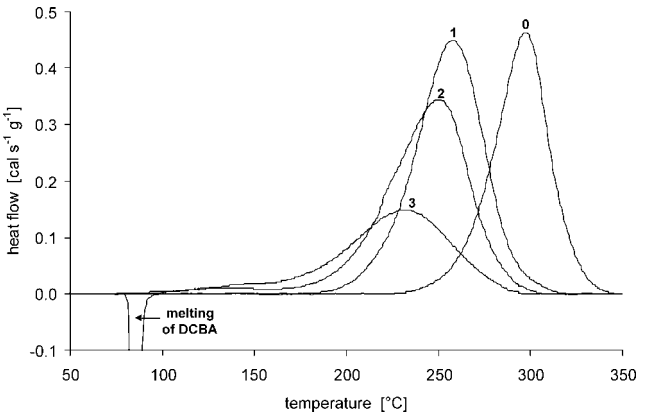

Figure 10 DSC curves (heating rate = 10 K/min) of (0) DCBA and (1–3) mixtures of DCBA with DMDPS [initial SH content = (1) 5, (2) 10, and (3) 20 mol %].

This behavior is similar to that found for other XH groups such as phenols[6,7] and primary amines,[8] for which a comparable reaction mechanism has been found. Furthermore, the acceleration of curing increases with the addition of increasing amounts of comonomers, and the exothermic peak becomes broader. Simultaneously, an exothermic peak at lower temperatures can be detected, which is more clearly pronounced for the DCBA/TP mixtures. It can be hypothesized that the mobility of TP within the network and, therefore, the reaction rate are much higher than those of DMDPS because the glass temperatures of the forming networks are significantly lower for admixtures of TP than for equal amounts of thiol groups of DMDPS.

Flame retardancy

As a result of cone calorimetry testing at a heat flux of 50 kW/m^2, it has been found that a coreaction of DCBA with DMDPS produces no substantial differ-

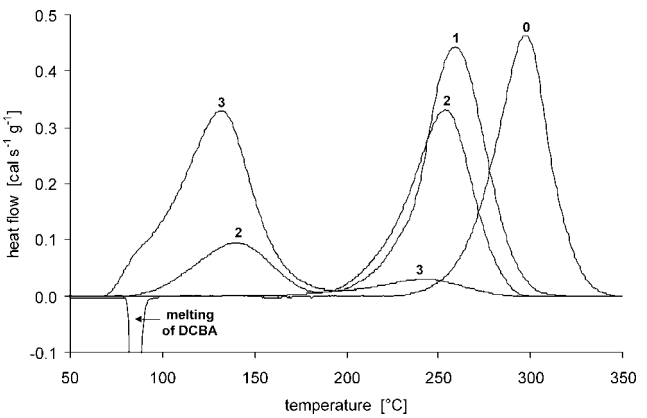

Figure 11 DSC curves (heating rate = 10 K/min) of (0) DCBA and (1–3) mixtures of DCBA with TP [initial SH content = (1) 2.6, (2) 11.1, and (3) 20.1 mol %].

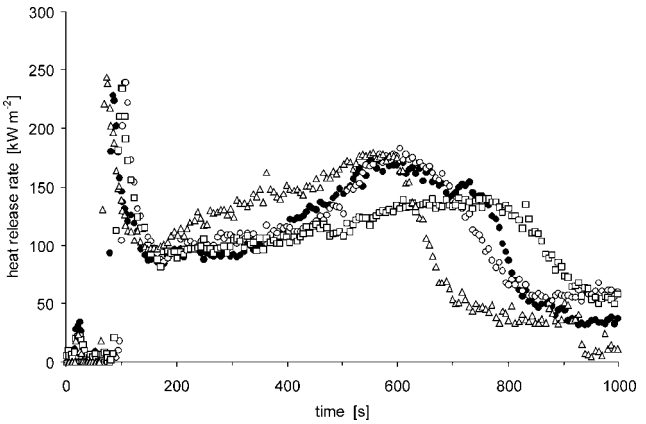

Figure 12 Heat release rates of DCBA/DMDPS thermosets measured by cone calorimetry: (●) neat DCBA, (○) 5 mol % initial SH content, (□) 10 mol % initial SH content, (△) 20 mol % initial SH content.

ences in the shape of the heat release rate curve, except for a reduction of the time to flameout and (unfortunately) time to ignition (Fig. 12). The time to flameout was reduced from 1000 to 833 s and the time to ignition was reduced from 93 to 60 s with the DMDPS content increasing from 5 to 20 mol %. The height of the peak does not show significant variations for tested samples and reaches about 240 kW/m^2. This result was also achieved with neat DCBA. Because of the formation of a protective carboneous barrier layer, the flame spread on the surface and release of decomposition products from samples were reduced. The heat release rate declined to about 100 kW/m^2 and was nearly the same for all samples. Sustained heat impact on the barrier layer and pressure from enclosed decomposition products caused swelling of the samples and cracks at the barrier layer. Combustion was reinforced again. The total heat release at flameout reached about the same value for all samples. Roughly two thirds of the initial resin mass was consumed during combustion.

CONCLUSIONS

The coreaction in bulk of cyanates and aromatic thiols was elucidated with monofunctional model compounds 4tbPC and TP with the help of HPLC, MALDI-TOF, and FTIR. It was found that the main reaction products were aryloxy- and arylthio-substituted 1,3,5-triazines; 4-*tert*-butyl phenol and DPDS were identified as byproducts. A straightforward three-step reaction was proposed and verified by the identification of key substances:

1. The addition of thiol and cyanate groups to form thioimino carbonic esters and the addition of phenol and cyanate groups to form imino carbonic esters.
2. The stepwise addition of (thio)imino carbonic esters to one another to form chain-extended (thio)imino carbonic esters.
3. The ring closure of chain-extended (thio)imino carbonic esters to form aryloxy- and arylthio-substituted 1,3,5-triazines.

Reactions of types 2 and 3 are associated with an abstraction of phenol or TP, which can enter reaction 1 again.

The network buildup resulting from the reaction in bulk of the difunctional cyanate DCBA with TP was also analyzed by MALDI-TOF. Series of oligomeric products differing in their structural composition by numbers of triazine rings and aryloxy or arylthio substituents and kinds of end groups were identified and completely confirmed the proposed reaction scheme (reactions 1–3).

Fully cured thermosets resulting from the reaction of DCBA with different admixtures of monofunctional TP as well as difunctional thiol DMDPS were characterized by DMA. It was found that large amounts of thiol comonomers (up to 20 mol %) could be incorporated into the network, which led to a lower glass temperature but a higher fracture toughness of the thermosets. Furthermore, the reaction rates were significantly enhanced by the admixture of thiols to the cyanate. The flame retardancy of fully cured DCBA/DMDPS thermosets was found to be only slightly influenced by the incorporation of DMDPS into the triazine network because unmodified polycyanurates with the high content of nitrogen exhibited high intrinsic flame retardancy.[10]

The authors thank S. Glaser for performing experiments and matrix-assisted laser desorption/ionization time-of-flight spectroscopy measurements and T. Mühlenberg for performing cone calorimetry measurements.

References

1. Grigat, E.; Pütter, R. Angew Chem 1967, 79, 219.
2. Martin, D.; Bacaloglu, R. Organische Synthesen mit Cyansäureestern; Akademie: Berlin, 1980.
3. Grigat, E.; Pütter, R. Chem Ber 1964, 97, 3022.
4. Martin, D.; Weise, A.; Niclas, H.-J.; Rackow, S. Chem Ber 1967, 100, 3756.
5. Martin, D.; Bauer, M. Org Synth 1983, 61, 35.
6. Bauer, J.; Alla, C.; Bauer, M.; Bloch, B. Acta Polym 1995, 46, 241.
7. Bauer, M.; Bauer, J. In Chemistry and Technology of Cyanate Ester Resins; Hamerton, I., Ed.; Blackie: Glasgow, 1994; p 58.
8. Bauer, J.; Bauer, M. Macromol Chem Phys 2001, 202, 2213.
9. Bauer, M.; Bauer, J.; Garske, B. Acta Polym 1986, 37, 604.
10. Hamerton, I. In Chemistry and Technology of Cyanate Ester Resins; Hamerton, I., Ed.; Blackie: Glasgow, 1994; p 205.